

Energy Management and Power Quality Enhancement of Hybrid Renewable Energy Generation System Using ANN-Based Coordinated Control Scheme

Yedla Sadha Siva¹, Kasarapu Sathish Kumar²

¹M.Tech (PSA), EEE, Sanketika Vidya Parishad Engineering College., India

²Assistant Professor, EEE, Sanketika Vidya Parishad Engineering college., India

E-mail: sadhasiva2001@gmail.com, sathishkumar342@gmail.com

ABSTRACT:

In modern electricity production, renewable energy sources like wind power systems and solar photovoltaic (PV) panels are increasingly used. The current and predicted weather patterns significantly impact these systems, causing irregular behavior that affects output and manufacturing. Consequently, timely adjustments in energy distribution and transmission networks are becoming more critical. This research introduces a new smart grid application for power system operation. To decrease undesirable harmonics, balance reactive power in the power sources, and enhance power quality and flow in the distribution system, a Static Compensator (STATCOM) device is utilized. The system connects a Three-Phase Four-Wire (3P4W) distribution network to a quasi-Z-Source Inverter (qZSI) based STATCOM. The proposed compensator circuit, which includes a PV system and a qZ-source, is used for switching purposes. An Adaptive Frequency Fixed (AFF) - Second Order Generalized Integrator (SOGI) operates the compensator. Optimization is achieved using a fuzzy logic controller (FLC) and Artificial Neural Networks (ANNs). The experimental outcomes demonstrate that the system effectively reduces the source current's Total Harmonic Distortion (THD) from 25.5% to 1.3%. Additionally, the technology has proven its capability to provide active power to the load.

1. INTRODUCTION:

The development of commercially feasible alternative means of producing electrical energy is significantly hampered by the rapid global growth in environmental deterioration. This has led to a large global research effort to find a way to produce a long-term, sustainable solution that is also environmentally beneficial in the area of generating electricity. The main players in the renewable energy generation sector include biomass, fuel cells, PV, and wind farms [1]. Wind-powered standalone systems have demonstrated their capacity to satisfy the electrical needs of a significant number of rural clients worldwide, making them a reliable energy source. Customers from carrying out the installation of renewable energy sources. There are many locations across the world where one may find plenty of solar energy, which can be paired with high or medium-high wind energy potential to reduce the requirement for energy storage in typical standalone systems [2].

Because of the significant variations in their availability throughout the day, individual solar and wind power use is typically unable to meet the fluctuating demands of the grid. Stand-alone solar and wind energy systems need to have a large amount of storage capacity in order to meet the energy needs of distant customers [3]. By utilizing the complementing characteristics of solar and wind power, it is feasible to lower the quantity of energy storage required in a system. Various types of distributed power production are widely acknowledged for microgrid applications. On the other hand, the typical inverter needs to be larger in order to handle the enormous fluctuations in PV array voltage caused by the low output voltage of the PV panels and the wide range of variation

dependent on temperature and irradiance, which is generally at a ratio of 1:1. The low voltage output of an inverter must be connected to the grid via huge low-frequency transformers; however, these transformers have a number of disadvantages, such as larger size, lower efficiency, increased acoustic noise, and higher total costs.

By employing a boost DC/DC converter to raise the input voltage from a wide range to the intended constant value, the two-stage inverter does away with the requirement for a transformer [7]. The DC/DC converter turns out to be the most costly and effective part of the system because of a broken switch. Galvanic isolation, which can be implemented on the AC output side of a line frequency transformer or in the DC/DC boost converter that uses a high-frequency transformer, is a feature of various solar-powered energy generation systems for increased safety [8]. Such additional galvanic isolations increase the overall cost and size of the system and decrease its overall efficacy. Transformer less topologies need more research because to their higher efficiency, smaller size, and lower cost for the PV system [9]. Because of its single-stage power converter for step-up and step-down functionalities, the qZSI has been employed in PV systems. Furthermore, the inverter can handle a wide variety of PV DC voltage fluctuations without being overpowered. This lowers the system's total cost, lowers the number of components and their expenses, and improves stability and dependability. PV systems may profit from a number of distinctive and fascinating advantages provided by qZSIs. By removing the need for additional filtering capacitors and drawing a stable current from the PV panel, the qZSI reduces switching ripples and streamlines the PV system. It also makes the PV system simpler and has a lower component rating (capacitor). This study interfaced the PV-generating equipment using qZSI for the isolated load situation. In order to improve the distribution system's power quality, the study's authors describe installing an AFF-SOGI control scheme in conjunction with a photovoltaic array and a qZSI-STATCOM that is backed by a Wind Energy Conversion System (WECS). The two are used in tandem to achieve this. These are the main objectives that this inquiry seeks to fulfil. Using an AFF-SOGI-based control algorithm to

regulate the qZSI-STATCOM can help enhance the power quality in the distribution system when there is a DC offset in the load currents together with distorted and unbalanced voltages. Thanks to the qZSI-STATCOM's multi-mode capabilities, this can be accomplished in the presence of both situations. Here is an outline of the paper's structure. Here is an outline of the paper's structure. Section II contains the system configuration. Section III provides an overview of the process for system modelling and control design. In part IV, experimental research is used to validate the suggested system. Section V concludes the paper.

2. SYSTEM CONFIGURATION:

Power generators, like wind turbines and photovoltaic cells, are used to supply the load more efficiently than any other power source due to their low cost and flexible operation. As a result, both linear and non-linear loads are dependent upon the wind turbine. Compensation circuits are employed in distribution networks to enhance power quality. In tandem with the distribution network is a STATCOM compensator based on a qZSI, which addresses the power quality problems at the source. In the proposed compensator circuit, the qZSI and PV system have been merged into one, and STATCOM is used for switching. Fig. 1 depicts the qZSIbased STATCOM model that has been presented.

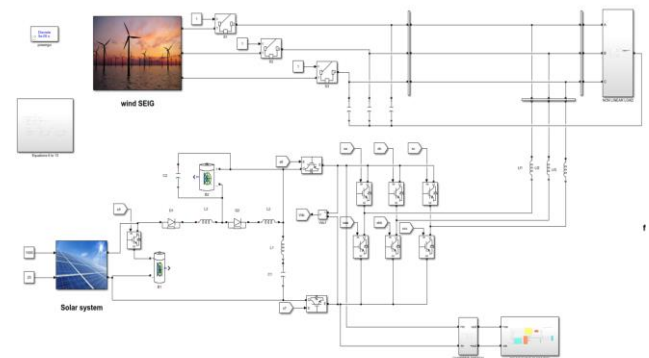


FIGURE 1. qZSI-STATCOM integrated with the wind energy conversion system.

The compensator is instructed by the AFF-SOGI control approach to maintain the voltage and frequency of the wind energy system within allowable bounds. This contributes to the 3P4W distribution system's harmonic attenuation as well. The frequency controller's parameters are optimized by the fuzzy-tuned PI controller. This method balances the reactive power from the power sources and removes harmonics to regulate the flow of power to the load. With coordinated control, this PV-assisted qZSI-STATCOM operates in four distinct modes.

The closed or open condition of the power system is shown by Modes 1 (PV power production), 2 (battery backup), 3 (continuous supply), and 4 (flywheel energy storage) electronic switches (S1–S7).

When the PV power producing system's output exceeds the amount of power that is generated by the system, the control system enters mode 1. linked up with the load (P_{Load}). The switches in this mode are set as follows: S1, S2, S3 = On, S4 = On (If battery's State of Charge (SOC) ≤ 50%), S5 = Off, S6, S7 = active. The control mechanism moves to mode 2 when the PV system's output of PV power falls to P_{PV} < 10%. V_{sabc} equals zero, which activates the mode: 3 setting. and the following switch locations are in place: S5, Off, S6, S7, S1, S2, S3, S4, S5, S4, S5 = On (If P_{PV} < 10%). When the control system determines that the power provided by the load (P_{Load}) is less than the power produced by the wind energy system (P_{wind}), it will enter mode 4. Figure 2 illustrates the state of transition from one mode to another.

I.AFF-SOGI CONTROL FOR qZSI-STATCOM:

The assistance of the qZSI-STATCOM control, harmonics may be reduced and reactive power consumption from connected loads can be made up for, improving the overall reliability of the power grid. Making the grid currents pure sinusoids at distorted load currents and imbalanced voltages is another objective. As a result, sinusoidal reference grid currents can be estimated using the AFF-SOGI regardless of distorted load currents or uneven grid voltages [11], [12]. The AFF-SOGI control scheme for qZSI-STATCOM is shown in Fig. 3. Only the fundamental frequency currents are taken into account

by AFF-SOGI. Where S/H stands for Sample and Hold circuit, Abs for Absolute, and ZCD for Zero Crossing Detector. It accomplishes this by only permitting currents produced by the other frequency component to enter the grid and preventing the other frequency component from producing the problematic currents. As a result, the system only draws active power from the source [13], [14]. Furthermore, the controller utilizes unit voltage vectors that are calculated using the positive sequence voltages in the grid.

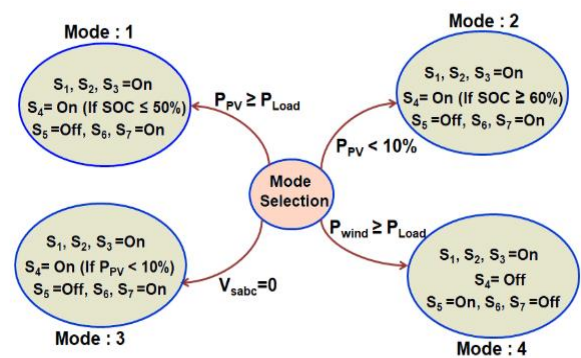


FIGURE 2. PV-assisted qZSI-STATCOM operating modes

This guarantees that the reference currents are unaffected by distortions and imbalances in the grid voltages. This technique replaces the damping factor and permits the extraction of the fundamental current. It is derived from a SOGI algorithm based on a constant frequency the resonant frequency using these values' fractional order versions [15], [16]. The addition of a DC offset rejection loop has greatly enhanced the AFF-SOGI. This loop ensures that the DC offsets in the load current no longer affect the fundamental current estimation [17]. The AFF-SOGI schematic, which shows how its internal components are arranged, is shown in Fig. 4.

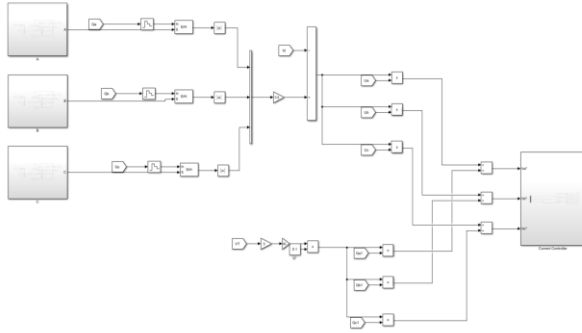


FIGURE 3. AFF-SOGI control scheme for qZSI-STATCOM.

The AFF-SOGI's in-quadrature transfer function can be defined using the following expression:

v' and q' represent the in-quadrature fundamental-frequency signals. The fractional order damping factor (m') and resonant frequency (n'), respectively, are represented. The notations v' and q' , respectively, represent the signals at the fundamental frequency. The resonant frequency can be represented by n' , and the fractional order damping factor by m' .

$$\frac{v'}{v} = \frac{mw_n s^2}{s^3 + (k_1 + mw_n)s^2 + (w_n)^2 s + k_1(w_n)^2} \quad (1)$$

$$\frac{q'}{v} = \frac{m(w_n)^2 s}{s^3 + (k_1 + ms_n)s^2 + (w_n)^2 s + k_1(w_n)^2} \quad (2)$$

$$m' = -2 \cos\left(\frac{\mu}{x}\right) \quad (3)$$

$$w'_n = w_n^{\frac{1}{2}} \quad (4)$$

$$\frac{\mu}{x} = \left\{ \pi - \frac{\sqrt{4-m^2}}{m}, 0 < m < 2\pi, m \geq 2 \right. \quad (5)$$

Even though the AFF-SOGI is optimized with respect to parameters m and n , it is based on the frequency fixed (FF)-SOGI. But if m' and n' are changed using x , AFF-SOGI might become sufficiently adaptive to manage changes in grid frequency. On the other hand, basic load currents can also be calculated using this method. Holding a sample of the estimated fundamental currents at each zero crossing of the quadrature unit vectors allows one to compute the active current.

To ascertain whether a signal has passed zero, utilize a ZCD. Unit vectors carrying grid voltage phase and frequency allow for synchronization through these vectors. Considering vectors should be pure sinusoids with a unit amplitude; distortion and unbalanced voltages have the potential to modify them [18], [19]. For this purpose, positive sequence voltages are used to form the unit vectors. The grid's phase voltages are listed below based on the highest current estimates that are available:

$$v = \frac{1}{3}(2v_{sabp} + v_{sbcp}) \quad (6)$$

$$v = \frac{1}{3}(-v_{sabp} + v_{sbcp}) \quad (7)$$

$$v_{sc} = \frac{1}{3}(-v_{sabp} + v_{sbcp}) \quad (8)$$

Let v_{sa} , v_{sb} , and v_{sc} be the grid phase voltages; v_{sab} , v_{sbc} , and v_{sca} be the grid line voltages. Let v_{sabp} , v_{sbcp} , and v_{scap} be the positive sequence line voltages of the grid. The following formula is used to calculate the amplitudes of PCC voltages, V_T , and unit templates in-phase and quadrature-phase:

$$V_T = \sqrt{\frac{2}{3}(V_{sa}^2 + V_{sb}^2 + V_{sc}^2)} \quad (9)$$

$$U_a = \frac{v_{sa}}{V_T}, U_b = \frac{v_{sb}}{V_T}, U_c = \frac{v_{sc}}{V_T} \quad (10)$$

$$q_a = \frac{U_a}{\sqrt{3}} + \frac{U_c}{\sqrt{3}} \quad (11)$$

$$q_b = \frac{\sqrt{3}U_a}{2} + \frac{(U_b - U_c)}{2\sqrt{3}} \quad (12)$$

$$q_c = \frac{\sqrt{3}U_a}{2} + \frac{(U_b - U_c)}{2\sqrt{3}} \quad (13)$$

Assume that the quadrature-phase unit templates are q_a , q_b , and q_c , while the in-phase unit templates are U_a , U_b , and U_c . The average active current when three phases of active currents are being used can be found using the following equation:

$$I_{p\ avg} = \frac{I_{pa} + I_{pb} + I_{pc}}{3} \tag{14}$$

A. FREQUENCY CONTROL:

The frequency of the system is determined by utilizing a Phase Locked Loop (PLL) using three-phase terminal voltages as input [20]. A fuzzy-tuned PI controller is used to compare the estimated frequency to the reference frequency and to control the frequency error. The active current that is drawn by the compensator circuitry constitutes the output of the frequency PI controller.

$$I_{d(n)} = I_{d(n-1)} + k_{pd}\{f_{er(n)} - f_{er(n-1)}\} + k_{id}f_{er(n)} \tag{15}$$

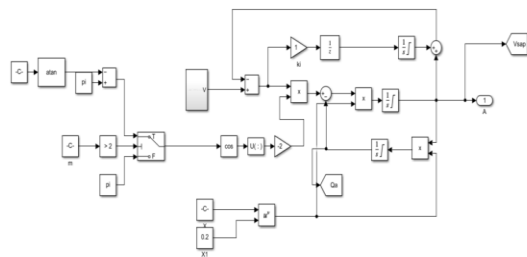


FIGURE 4. Internal structure of AFF-SOGI

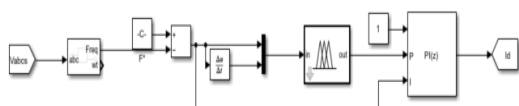


FIGURE 5: Fuzzy-tuned PI frequency controller

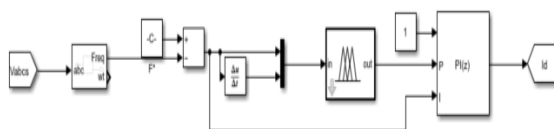


FIGURE 6: DC link voltage controller

The frequency difference between the measured frequency of the terminal voltage ($f_{er}(n)$) and the reference frequency of the terminal voltage ($f \setminus$) is indicated for each sampling instant by the formula $f_{er}(n) = f \setminus - f(n)$. K_{id} and K_{pd} stand for the proportional and integral gains, respectively, for the frequency PI controller. The PI controller gain parameters are adjusted using the fuzzy-tuned PI controller. Fig. 5 displays the fuzzy-tuned PI frequency controller. Equations (16) and (17) specify that the K_P and K_I PI controller parameters must be changed at each time step k .

$$k_p(k + 1) = k_p(k) + \Delta k_p(k) \tag{16}$$

$$k_I(k + 1) = k_I(k) + \Delta k_I(k) \tag{17}$$

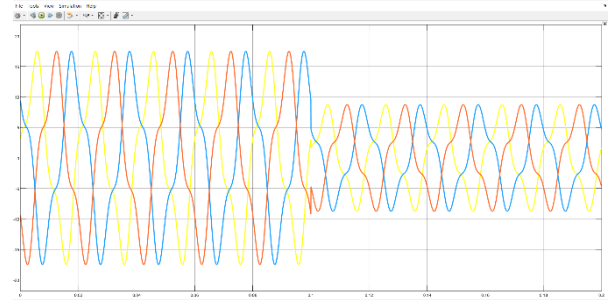
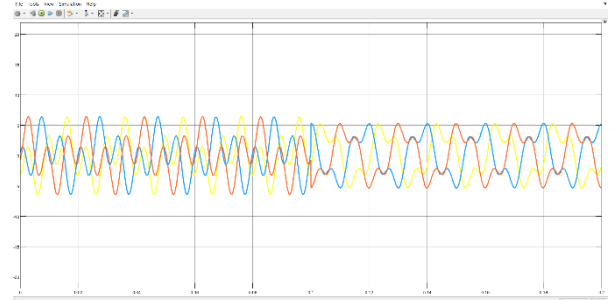
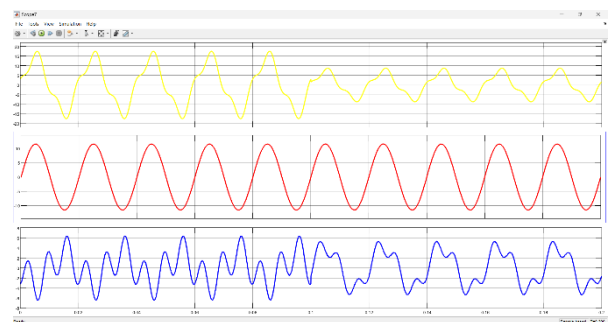


FIGURE 7. Case 1 compensation experimental results: (a) Balanced load current (ILabc) (b) Load, source, and injected current (c) Current at the source side (ISabc).

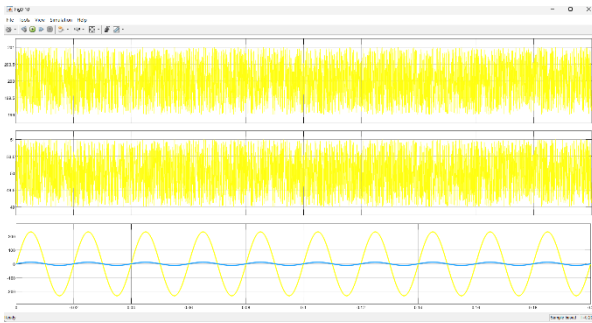


FIGURE 8. Voltage at DC link (Vdc), Voltage of PV array (VPV) and Source voltage and current.



FIGURE 9. Controlling the DC-link voltage's dynamic aspects: (a) The voltage of the DC-link if the load current decreases (b) Voltage of the DC link with a rise in load current.

Each rule table has 15 rules, and the implementation results confirm that the computing cost is within tolerable bounds. The following is the implication of their statement:

For example, if e is represented by the A_i and E_c by the B_j , then $1KP/1KI$ is C_{ij}/D_{ij} , where the A_i , B_j , C_{ij} and D_{ij} are related to the fuzzy subsets of e , E_c , $1KP$ and $1KI$. To accomplish fuzzy inference, Mamdani's Min-Max approach is employed. Using the fuzzy subsets C_{ij} , the degree of membership for the parameter $1KP$ may be calculated as follows:

$$u_c(\Delta K_p) = \bigwedge_{i,j=1}^7 \{ [u_i(e) \wedge u_j(de)] \wedge u_{cij}(\Delta K_p) \} \quad (18)$$

The symbol $u(x)$ represents the degree of membership. Defuzzification is the process of converting fuzzy variables into discrete values or integers in computing. The centre of gravity strategy must be used in order to achieve critical values. The parameter KP , which is equivalent to KI , may be found using the following equation:

$$\Delta K_p(e, de) = \frac{\sum_{k=1}^7 \Delta k_p u_c(\Delta K_p)}{\sum_{k=1}^7 u_c(\Delta K_p)} \quad (19)$$

The PI DC-link controller gives the power electronic switch $S5$ a gating pulse that powers the flywheel energy storage device.

B. FREQUENCY CONTROL USING ANN:

The frequency of the system is determined by utilizing a Phase Locked Loop (PLL) using three-phase terminal voltages as input. The ANN controller is trained to compare the estimated frequency to the reference frequency and to control the frequency error. The active current drawn by the compensator circuitry constitutes the output of the ANN controller.

C. DC LINK VOLTAGE CONTROL USING ANN:

The DC link voltage control is handled by an ANN that replaces the traditional PI controller. The inputs to the ANN include the error in DC link voltage ($V_{dc} - V_{dc}^* - V_{dc}$) and the change in error. The ANN outputs the gating pulses for the power electronic switches to regulate the DC link voltage.

D. Design of the ANN Controller for DC Link Voltage:

Similar to the frequency control, the ANN controller for DC link voltage includes input layers, hidden layers, and an output layer. The inputs to the ANN are the error in voltage and the change in error.

3. SIMULATION VALIDATION:

Using a simulation, the output of the PV-aided STATCOM with AFF - SOGI controller is tested under various load conditions. In each of the

situations, the system's feasibility was evaluated. Below are a number of case studies illustrating the results of experimental prototypes. A list of the system parameters used in the experiment is provided in Table 1.

CASE 1: BALANCED NON-LINEAR LOADS AT CONSTANT WIND SPEED:

PV-STATCOM is assessed under the conditions of a constant wind speed and balanced non-linear loads. The current compensation experimental results for Case 1 compensation are displayed in Fig. 7. A constant voltage and current can be maintained by using the compensator circuit, even though the non-linear balanced load has an impact. Fig. 8 displays the experimental findings for the DC link voltage, PV array voltage, source voltage, and current.

It is feasible to assess the dynamic characteristics of DC-link voltage management by changing the load current. Figure 9(a) depicts the DC-link voltage when the load current is increased, and Figure 9(b) shows the DC-link voltage when the load current is dropped. As the load current increases, the DC link voltage reduces, and as the load current declines, the DC link voltage rises. The harmonic spectrum for the uncompensated source current is shown in Fig. 10. The integration of the qZSI-STATCOM reduces the THD for compensated source current from 25.6%, 25.4%, and 25.5% to 1.3%, 1.4%, and 1.3%, respectively, as shown in Fig. 11.

CASE 2: BALANCED LOAD CURRENT WITH VARYING WIND SPEED:

It illustrates how the grid current becomes sinusoidal and stays in phase with the phase voltage as soon as the qZSI-STATCOM is turned on. This usually leads to an operation with a power factor of unity. Uncompensated load current and compensated source current with compensator circuitry are shown in Fig. 12.

Figure 13 displays the DC-link voltage and PV array voltage of the qZSI-based PV-STATCOM. Figs. 14 and 15, respectively, show the source current's THD both before and after adjustment. It has been observed

that following adjustment, the source current's THD decreases from 25.2%, 25.4%, and 25.5% to 1.3%, 1.4%, and 1.3%, respectively. Because of this, STATCOM, which is based on AFF-SOGI, can effectively correct the load current's harmonics even in situations when the wind speed varies.

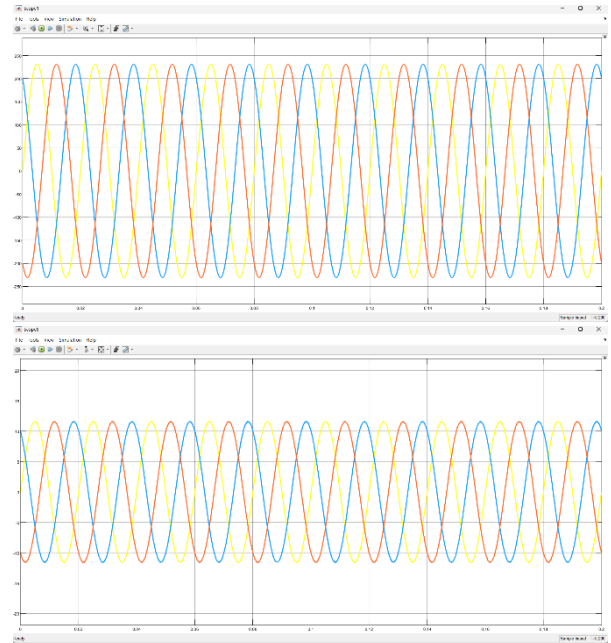


FIGURE 12. Experimental results of (a) Uncompensated current (b) Compensated source current.

4. CONCLUSION:

The key players in the power industry have acknowledged the significant contribution that FACTS has made to the enhancement of power system quality. Additionally, because of the characteristics of STATCOM devices, it is possible to integrate qZSI-STATCOM devices with renewable energy facilities. Enhancing transient stability, voltage tripping, and power flow management are a few of these characteristics; these are all necessary for the operation of wind and solar power plants. The surrounding area's climate has a significant impact on these systems. The system's erratic behaviour has an impact on the range of output and production values. Consequently,

a new smart grid application has been created to be used in power system management in order to control power flow, increase capacities, reduce distribution system harmonics, and correct for power source-induced voltage disruptions. The technique given allows for improvements in the qZSI STATCOM's performance when modifications are made using the fuzzy-tuned PI controller. By determining the perfect values for the PI controller gains, the voltage fluctuation caused by the change in reactive power has been minimized, harmonics have been reduced, and the desired dynamic response has been achieved.

A comparison of several FACTS devices and optimization methodologies may be conducted in later study to determine which is the most effective. The measurement of 1.3% for the source current's THD was noted by the researchers.

This value is less than the THD that a traditional STATCOM and the control scheme that goes along with it display.

REFERENCES

- [1] L. de Oliveira-Assis, P. García-Triviño, E. P. P. Soares-Ramos, R. Sarrias-Mena, C. A. García-Vázquez, C. E. Ugalde-Loo, and L. M. Fernández-Ramírez, "Optimal energy management system using biogeography based optimization for grid-connected MVDC microgrid with photovoltaic, hydrogen system, electric vehicles and Z-source converters," *Energy Convers. Manage.*, vol. 248, Nov. 2021, Art. no. 114808, doi: 10.1016/j.enconman.2021.114808.
- [2] S. Ouchen, A. Betka, S. Abdeddaim, and A. Menadi, "Fuzzy-predictive direct power control implementation of a grid connected photovoltaic system, associated with an active power filter," *Energy Convers. Manage.*, vol. 122, pp. 515–525, Aug. 2016, doi: 10.1016/j.enconman.2016.06.018.
- [3] P. Aree, "Dynamic performance of self-excited induction generator with electronic load controller under starting of induction motor load," in *Proc. 5th Int. Conf. Electr., Electron. Inf. Eng. (ICEEIE)*, Malang, Indonesia, Oct. 2017, pp. 21–24, doi: 10.1109/ICEEIE.2017.8328756.
- [4] A. B. Shitole, H. M. Suryawanshi, G. G. Talapur, S. Sathyan, M. S. Ballal, V. B. Borghate, M. R. Ramteke, and M. A. Chaudhari, "Grid interfaced distributed generation system with modified current control loop using adaptive synchronization technique," *IEEE Trans. Ind. Informat.*, vol. 13, no. 5, pp. 2634–2644, Oct. 2017, doi: 10.1109/TII.2017.2665477.
- [5] H. Abu-Rub, A. Iqbal, S. M. Ahmed, F. Z. Peng, Y. Li, and G. Baoming, "Quasi-Z-source inverter-based photovoltaic generation system with maximum power tracking control using ANFIS," *IEEE Trans. Sustain. Energy*, vol. 4, no. 1, pp. 11–20, Jan. 2013, doi: 10.1109/TSTE.2012.2196059.
- [6] J. Zhang, "Unified control of Z-source grid-connected photovoltaic system with reactive power compensation and harmonics restraint: Design and application," *IET Renew. Power Gener.*, vol. 12, no. 4, pp. 422–429, Mar. 2018, doi: 10.1049/iet-rpg.2016.0478.
- [7] J. G. Cintron-Rivera, Y. Li, S. Jiang, and F. Z. Peng, "Quasi-Z- source inverter with energy storage for photovoltaic power generation systems," in *Proc. 26th Annu. IEEE Appl. Power Electron. Conf. Expo. (APEC)*, Fort Worth, TX, USA, Mar. 2011, pp. 401–406, doi: 10.1109/APEC.2011.5744628.
- [8] N. Cheraghi Shirazi, A. Jannesari, and P. Torkzadeh, "Self-start-up fully integrated DC–DC step-up converter using body biasing technique for energy harvesting applications," *AEU-Int. J. Electron. Commun.*, vol. 95, pp. 24–35, Oct. 2018, doi: 10.1016/j.aeue.2018.07.033.
- [9] S. Parthiban and V. Madhaiyan, "Experimental validation of solar PV sustained ZSI based unified active power filter for enrichment of power quality," *Automatika*, vol. 62, no. 1, pp. 137–153, Jan. 2021, doi: 10.1080/00051144.2021.1908013.
- [10] M. Vijayakumar and S. Vijayan, "PV based three-level NPC shunt active power filter with extended reference current generation method," *Int. J. Electr. Energy*, vol. 2, no. 4, pp. 258–267, 2014, doi: 10.12720/ijoee.2.4.258-267.
- [11] M. Vijayakumar and S. Vijayan, "A novel reference current generation method of PV based three

- level NPC shunt active power filter,” UPB Sci. Bull. C, vol. 77, no. 3, pp. 235–250, 2015.
- [12] A. K. K. Giri, S. R. Arya, R. Maurya, and B. C. Babu, “Power quality improvement in stand-alone SEIG-based distributed generation system using Lorentzian norm adaptive filter,” *IEEE Trans. Ind. Appl.*, vol. 54, no. 5, pp. 5256–5266, Sep. 2018, doi: 10.1109/TIA.2018.2812867.
- [13] M. Ahmed, M. Orabi, S. Ghoneim, M. Alharthi, F. Salem, B. Alamri and S. Mekhilef, “Selective harmonic elimination method for unequal DC sources of multilevel inverters,” *Automatika*, vol. 60, no. 4, pp. 378–384, Oct. 2019, doi: 10.1080/00051144.2019.1621048.
- [14] K. Patil and H. H. Patel, “Modified SOGI based shunt active power filter to tackle various grid voltage abnormalities,” *Eng. Sci. Technol., Int. J.*, vol. 20, no. 5, pp. 1466–1474, Oct. 2017, doi: 10.1016/j.jestch.2017.10.004.
- [15] B. Singh, S. Kumar, and C. Jain, “Damped-SOGI-based control algorithm for solar PV power generating system,” *IEEE Trans. Ind. Appl.*, vol. 53, no. 3, pp. 1780–1788, May/Jun. 2017, doi: 10.1109/TIA.2017.2677358.
- [16] J. A. Barrado, R. Grino, and H. Valderrama-Blavi, “Power-quality improvement of a stand-alone induction generator using a STATCOM with battery energy storage system,” *IEEE Trans. Power Del.*, vol. 25, no. 4, pp. 2734–2741, Oct. 2010, doi: 10.1109/TPWRD.2010.2051565.
- [17] F. U. Nazir, N. Kumar, B. C. Pal, B. Singh, and B. K. Panigrahi, “Enhanced SOGI controller for weak grid integrated solar PV system,” *IEEE Trans. Energy Convers.*, vol. 35, no. 3, pp. 1208–1217, Sep. 2020, doi: 10.1109/TEC.2020.2990866.
- [18] S. Senguttuvan and M. Vijayakumar, “Solar photovoltaic system inter- faced shunt active power filter for enhancement of power quality in three-phase distribution system,” *J. Circuits, Syst. Comput.*, vol. 27, no. 11, Oct. 2018, Art. no. 1850166, doi: 10.1142/S0218126618501669.
- [19] T. Jayakumar and A. A. Stonier, “Implementation of solar PV system unified ZSI-based dynamic voltage restorer with U-SOGI control scheme for power quality improvement,” *Automatika*, vol. 61, no. 3, pp. 371–387, Jul. 2020, doi: 10.1080/00051144.2020.1760591.
- [20] M. Ghanaatian and S. Lotfifard, “Control of flywheel energy storage systems in the presence of uncertainties,” *IEEE Trans. Sustain. Energy*, vol. 10, no. 1, pp. 36–45, Jan. 2019, doi: 10.1109/TSTE.2018.2822281.
- [21] K. Muthuvel and M. Vijayakumar, “Solar PV sustained quasi Z-source network-based unified power quality conditioner for enhancement of power quality,” *Energies*, vol. 13, no. 10, p. 2657, May 2020, doi: 10.3390/en13102657.
- [22] M. Hanif, M. Basu, and K. Gaughan, “Understanding the operation of a Z-source inverter for photovoltaic application with a design example,” *IET Power Electron.*, vol. 4, no. 3, pp. 278–287, 2011, doi: 10.1049/iet-pel.2009.0176.
- [23] IEEE Recommended Practice and Requirements for Harmonic Control in Electric Power Systems, *IEEE Standard 519-2014 (Revision of IEEE Std 519-1992)*, 2014, pp. 1–29, doi: 10.1109/IEEESTD.2014.6826459.
- [24] F. S. Ahmed, A. N. Hussain, and A. J. Ali, “Power quality improvement by using multiple sources of PV and battery for DSTATCOM based on coordinated design,” *IOP Conf. Ser., Mater. Sci. Eng.*, vol. 745, no. 1, Feb. 2020, Art. no. 012025, doi: 10.1088/1757-899X/745/1/012025.
- [25] L. Popavath and P. Kaliannan, “Photovoltaic-STATCOM with low voltage ride through strategy and power quality enhancement in a grid integrated wind-PV system,” *Electronics*, vol. 7, no. 4, p. 51, Apr. 2018, doi: 10.3390/electronics7040051.
- [26] L. Ashok Kumar and V. Indragandhi, “Power quality improvement of grid-connected wind energy system using facts devices,” *Int. J. Ambient Energy*, vol. 41, no. 6, pp. 631–640, May 2020, doi: 10.1080/01430750.2018.1484801.